ELSEVIER

A new technique for identification of eighteen flutter derivatives using a three-degree-of-freedom section model

Arindam Gan Chowdhury, Partha P. Sarkar *

Iowa State University, Department of Aerospace Engineering, 2271 Howe Hall, Ames, IA, 50011-2271, USA

Abstract

The prediction of flutter instability is of major concern for design of flexible structures. This necessitates the identification of aeroelastic parameters, known as flutter derivatives from wind tunnel experiments. The extraction of flutter derivatives becomes more challenging when the number of degrees of freedom (DOF) increases from two to three. Since the work in the field of identifying all 18 flutter derivatives has been limited, it has motivated the development of a new system identification method (iterative least squares method or ILS method) to efficiently extract the flutter derivatives using a section model suspended by a three-DOF elastic suspension system. The accuracy of a particular flutter derivative was determined by comparing the results obtained from all possible DOF combinations.
© 2003 Elsevier Ltd. All rights reserved.

1. Introduction

The discipline of aeroelasticity refers to the study of phenomenon wherein aerodynamic forces and structural motions interact significantly. Flutter is an aeroelastic self-excited oscillation of a structural system. Since the flutter-induced failure of the Tacoma Narrows Bridge in 1940, understanding of the physical mechanisms at work has advanced. The frequency-domain approach has been widely used for estimating flutter speed of structures [1,2]. The frequency-domain method uses flutter derivatives, which may be experimentally obtained from wind-tunnel testing of section models. Extraction of flutter derivatives can be done through the forced vibration technique or the free vibration technique. The free vibration technique is comparatively simple because it only requires initial displacements.

Sarkar [3] developed the modified Ibrahim time domain (MITD) method to extract all the direct and cross-flutter derivatives from the coupled free vibration data of a two-degree-of-freedom (DOF) section model. Sarkar et al.

[4,5] were successful in identifying eight flutter derivatives simultaneously from noisy displacement time-histories generated under laminar and turbulent flow.

Other system identification (SID) methods that can be applied to problems in structural dynamics are least squares (LS), instrumental variable (IV), maximum likelihood (ML), and extended Kalman filtering (EKF); these have been reviewed by Imai et al. [6]. Hsia [7] described different least squares algorithms for system parameter identification. Extended Kalman filtering techniques were used by Yamada and Ichikawa [8], Diana et al. [9], Iwamoto and Fujino [10] and Jones et al. [11]. Jakobsen and Hjorth-Hansen [12] and Brownjohn and Jakobsen [13] have used covariance block Hankel matrix (CBHM) method for parameter extraction of a two-DOF system. The CBHM method has also been extended to cater for three-DOF flutter derivatives. However the principles were illustrated for a two-DOF system and eight flutter derivatives were experimentally extracted [12,13]. Gu et al. [14] and Zhu et al. [15] have used an identification method based on unifying least squares (ULS) theory to extract flutter derivatives of a two-DOF model. Though the ULS method could theoretically identify all 18 flutter derivatives using a three-DOF section model, only eight flutter derivatives were extracted due to lack of a more

* Corresponding author. Tel.: +1-515-294-0719; fax: +1-515-294-3262.
E-mail address: ppsarkar@iastate.edu (P.P. Sarkar).

inclusive experimental set-up to accommodate the three-DOF section model (as quoted in [15]).

Eight flutter derivatives, namely, H1∗, H2∗, H3∗, H4∗, A1∗, A2∗, A3∗, and A4∗, can be obtained from two-DOF section model tests with vertical and torsional degree of freedom. The problem of flutter derivative extraction becomes more challenging when the number of DOF increases from two to three. The additional flutter derivates that can be extracted from three-DOF section model with vertical, torsional, and lateral degree of freedom are H5∗, H6∗, A5∗, A6∗, P1∗, P2∗, P3∗, P4∗, P5∗, and P6∗. Out of the 18 flutter derivatives, H1∗, H4∗, P1∗, P4∗, A2∗, and A3∗, are the direct flutter derivatives and the remaining 12 are the indirect flutter derivatives. The indirect flutter derivatives are more difficult to identify than the direct ones. Singh et al. [16] were the first researchers to attempt identification of all 18 flutter derivatives of a streamlined bridge deck. They extended the MITD method developed by Sarkar [3], that was already proven to work for a two-DOF system. The trend of some of the indirect flutter derivatives in [16], namely, H6∗, A5∗, A6∗, P3∗, P5∗, and P6∗, are difficult to predict due to the scatter in the data presented in the plots; for the other flutter derivatives, specific trends are evident from the plots. Chen et al. [17] have used general least-squares theory for identifying 18 flutter derivatives of bridge sections. The trends of experimental results were compared to results from computational fluid dynamics (CFD) methods. For the lateral flutter derivatives, the experimental results were consistent with the CFD results at lower reduced velocities. At higher velocities, the results of most lateral derivatives were different between both approaches. While comparing two-DOF and three-DOF sectional model experiments, good agreement was found for flutter derivatives H1∗, H2∗, H3∗, A1∗, A2∗, A3∗, but deviations were noted for H4∗ and A4∗.

The work in the field of identifying all 18 flutter derivatives for section models is limited and needs further investigation. The art of efficient extraction of all 18 flutter derivatives requires an effective system identification technique and a versatile three-DOF elastic suspension system. The system identification technique is required to perform accurate parameter extraction for high noise-to-signal ratio. A versatile three-DOF elastic suspension system is needed to capture coupled displacement time-histories from wind tunnel testing of section models. Comparison of results obtained from all possible DOF combinations can be an effective tool to measure the accuracy of flutter derivatives. Also, as parameter extraction through three-DOF testing is one magnitude more difficult than parameter extraction through two-DOF testing. Separate two-DOF combinations can be used to generate all 18 flutter derivatives, thus eliminating the need to perform three-DOF testing. Thus, an efficient three-DOF suspension system is highly advan-

tageous to simulate different DOF combinations that are needed for flutter derivative extraction. The current paper describes the development of a new system identification method and a versatile three-DOF elastic suspension system, which together are capable of efficiently extracting all 18 flutter derivatives for section models involving different DOF-combination testing. The flutter derivative nomenclature convention in this paper is consistent with that used by Scanlan and co-workers [16]. The system identification method involves digital filtering of noisy displacement time-histories and approximation of their higher derivatives using finite difference formulation. The current formulation has the following advantages: (1) a single computer program is capable of extracting flutter derivatives for various DOF combination cases (e.g. 1-DOF, 2-DOF, and 3-DOF cases); (2) effective stiffness and damping matrices are directly obtained from acquired free-vibration displacement time-histories and numerically generated velocity and acceleration time-histories using digital filtering and finite differencing (thus avoiding extraction of eigenvalues and eigenvectors); and (3) accurate parameter identification can be performed, as has been validated numerically and experimentally, where different DOF combinations were used.

2. Current system identification method

2.1. Equations of motion

Flutter analysis is performed by using experimentally obtained flutter derivatives in the frequency domain. In this formulation, the aeroelastic forces acting on a structure are modeled by means of flutter derivatives. Fig. 1 shows a typical section model that is subjected to a mean wind speed U.

The three degree of freedom are the vertical deflection h, and the horizontal deflection p of the local center-of-gravity (c.g.), and the rotation α about that c.g. The aerodynamic forces acting on the section are lift (L), drag (D), and moment (M). The section model has m_h, m_p, and I_α as vertical mass, lateral mass, and mass moment of inertia per unit length, respectively; ζ_h, ζ_p,
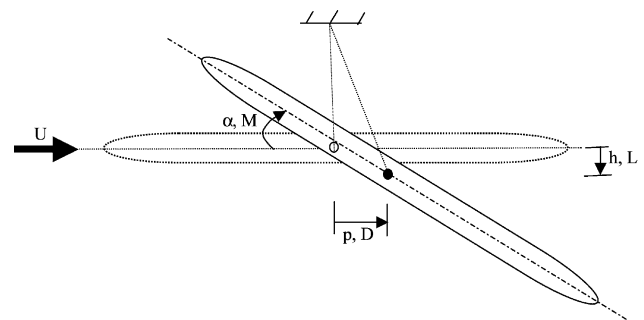

Fig. 1. Degree of freedom for a wing or deck section.

and ζ_α as the mechanical damping ratios, and ω_h, ω_p, and ω_α as the natural mechanical frequencies for vertical, lateral and torsional motion, respectively. The equations of motion for the section model subjected to aeroelatic forces can be written as:

$$\ddot{\underline{y}} + \underline{M}^{-1}\underline{C}\dot{\underline{y}} + \underline{M}^{-1}\underline{K}\underline{y} = \underline{M}^{-1}\underline{F}_{ae} \tag{1}$$

where

$$\underline{y} = \{h \ \alpha \ p\}^T, \underline{M} = \begin{bmatrix} m_h & 0 & 0 \\ 0 & I_\alpha & 0 \\ 0 & 0 & m_p \end{bmatrix}, \underline{M}^{-1}\underline{C}$$

$$= \begin{bmatrix} 2s_h\omega_h & 0 & 0 \\ 0 & 2s_\alpha\omega_\alpha & 0 \\ 0 & 0 & 2s_p\omega_p \end{bmatrix}, \underline{M}^{-1}\underline{K} = \begin{bmatrix} \omega_h^2 & 0 & 0 \\ 0 & \omega_\alpha^2 & 0 \\ 0 & 0 & \omega_p^2 \end{bmatrix}.$$

The aeroelastic force vector can be written as follows:

$$\underline{F}_{ae} = \begin{Bmatrix} L_{ae} \\ M_{ae} \\ D_{ae} \end{Bmatrix} = \begin{bmatrix} 0.5\rho U^2 B & 0 & 0 \\ 0 & 0.5\rho U^2 B^2 & 0 \\ 0 & 0 & 0.5\rho U^2 B \end{bmatrix}. \tag{2}$$

$$\begin{bmatrix} KH_1^*/U & KH_2^*B/U & KH_5^*/U & K^2H_4^*/B & K^2H_3^* & K^2H_6^*/B \\ KA_1^*/U & KA_2^*B/U & KA_5^*/U & K^2A_4^*/B & K^2A_3^* & K^2A_6^*/B \\ KP_5^*/U & KP_2^*B/U & KP_1^*/U & K^2P_6^*/B & K^2P_3^* & K^2P_4^*/B \end{bmatrix} \begin{Bmatrix} \dot{h} \\ \dot{\alpha} \\ \dot{p} \\ h \\ \alpha \\ p \end{Bmatrix}.$$

where ρ is the air density; U is the mean cross wind velocity; $K = B\omega/U$ is the non-dimensional reduced frequency; ω is the circular frequency oscillation.

The non-dimensional aerodynamic coefficients H_i^*, P_i^*, and A_i^* ($i = 1, 2, …, 6$) are called the flutter derivatives and they evolve as functions of the reduced velocity U/nB (where $n = \omega/2\pi$ is the frequency oscillation). Flutter instability of structures can be assessed analytically using the flutter derivative formulation and a set of flutter-derivative coefficients is used for this purpose. These coefficients can be determined from wind-tunnel experiments on section models excited by initial displacements.

2.2. Flutter derivatives

Substituting Eq. (2) in Eq. (1) and bringing all terms to the left hand side, aeroelastically modified free-vibration equations of motion are obtained:

$$\ddot{\underline{y}} + \underline{C}^{eff}\dot{\underline{y}} + \underline{K}^{eff}\underline{y} = \underline{0} \tag{3}$$

where C^{eff} and K^{eff} are the aeroelastically modified effective damping and stiffness matrices, respectively. For zero wind speed, the mechanical damping and stiffness matrices are C^{mech} and K^{mech}, respectively. The expression of flutter derivatives obtained from a three-DOF section model can be written as:

$$H_1^*(K) = -\frac{2m_h}{\rho B^2 \omega}(C_{11}^{eff}-C_{11}^{mech}) \tag{4a}$$

$$H_2^*(K) = -\frac{2m_h}{\rho B^3 \omega}(C_{12}^{eff}-C_{12}^{mech}) \tag{4b}$$

$$H_3^*(K) = -\frac{2m_h}{\rho B^3 \omega^2}(K_{12}^{eff}-K_{12}^{mech}) \tag{4c}$$

$$H_4^*(K) = -\frac{2m_h}{\rho B^2 \omega^2}(K_{11}^{eff}-K_{11}^{mech}) \tag{4d}$$

$$H_5^*(K) = -\frac{2m_h}{\rho B^2 \omega}(C_{13}^{eff}-C_{13}^{mech}) \tag{4e}$$

$$H_6^*(K) = -\frac{2m_h}{\rho B^2 \omega^2}(K_{13}^{eff}-K_{13}^{mech}) \tag{4f}$$

$$A_1^*(K) = -\frac{2I_\alpha}{\rho B^3 \omega}(C_{21}^{eff}-C_{21}^{mech}) \tag{5a}$$

$$A_2^*(K) = -\frac{2I_\alpha}{\rho B^4 \omega}(C_{22}^{eff}-C_{22}^{mech}) \tag{5b}$$

$$A_3^*(K) = -\frac{2I_\alpha}{\rho B^4 \omega^2}(K_{22}^{eff}-K_{22}^{mech}) \tag{5c}$$

$$A_4^*(K) = -\frac{2I_\alpha}{\rho B^3 \omega^2}(K_{21}^{eff}-K_{21}^{mech}) \tag{5d}$$

$$A_5^*(K) = -\frac{2I_\alpha}{\rho B^3 \omega}(C_{23}^{eff}-C_{23}^{mech}) \tag{5e}$$

$$A_6^*(K) = -\frac{2I_\alpha}{\rho B^3 \omega^2}(K_{23}^{eff}-K_{23}^{mech}) \tag{5f}$$

$$P_1^*(K) = -\frac{2m_p}{\rho B^2 \omega}(C_{33}^{eff}-C_{33}^{mech}) \tag{6a}$$

$$P_2^*(K) = -\frac{2m_p}{\rho B^3 \omega}(C_{32}^{eff}-C_{32}^{mech}) \tag{6b}$$

$$P_3^*(K) = -\frac{2m_p}{\rho B^3 \omega^2}(K_{32}^{eff}-K_{32}^{mech}) \tag{6c}$$

$$P_4^*(K) = -\frac{2m_p}{\rho B^2 \omega^2}(K_{33}^{eff}-K_{33}^{mech}) \tag{6d}$$

$$P_5^*(K) = -\frac{2m_p}{\rho B^2 \omega}(C_{31}^{eff}-C_{31}^{mech}) \tag{6e}$$

$$P_6^*(K) = -\frac{2m_p}{\rho B^2 \omega^2}(K_{31}^{eff}-K_{31}^{mech}). \tag{6f}$$

2.3. Iterative least squares method

A new system identification technique has been developed for the extraction of flutter derivatives from free vibration displacement time-histories obtained from a section model tested in a wind tunnel. The method uses an iterative least squares system identification approach and will be referred to hereafter as the iterative least squares (ILS) method. The detailed formulation of the ILS method is discussed in this Section. Eq. (3) can be represented as the state-space model:

$$\underline{\dot{X}} = \underline{A}\underline{X} \tag{7}$$

where

$$\underline{X} = \begin{Bmatrix} y \\ \dot{y} \end{Bmatrix}, \underline{A} = \begin{bmatrix} \underline{0} & \underline{I} \\ -\underline{K}^{eff} & -\underline{C}^{eff} \end{bmatrix}.$$

The *A* matrix is $2n \times 2n$ square matrix, where *n* is the number of degree of freedom for the dynamic system; *I* is the identity matrix of size $n \times n$. The *A* matrix can be identified if acceleration, velocity and displacement data can be recorded for all *n* degree of freedom for at least $2n$ different instants of time [18]. In practice, measurement of all three responses is not feasible. Thus, an alternative arrangement can be designed in which the noisy *displacement* time-history is only measured and filtered numerically to remove the high frequency noise components (if any). This *filtered displacement* data can then be used to generate *velocity* and *acceleration* time-histories by finite difference formulation. For numerical simulation, a noise-free vertical displacement time-history (referred to as actual displacement time-history) was contaminated with Gaussian white noise and the noisy time-history is shown in Fig. 2. MATLAB was used for zero-phase digital filtering of the noisy displacement time-history. A low-pass digital 'Butterworth' filter was built for this purpose. The
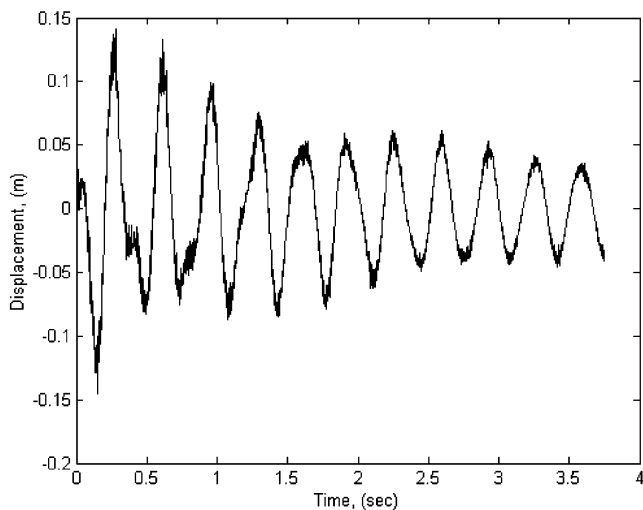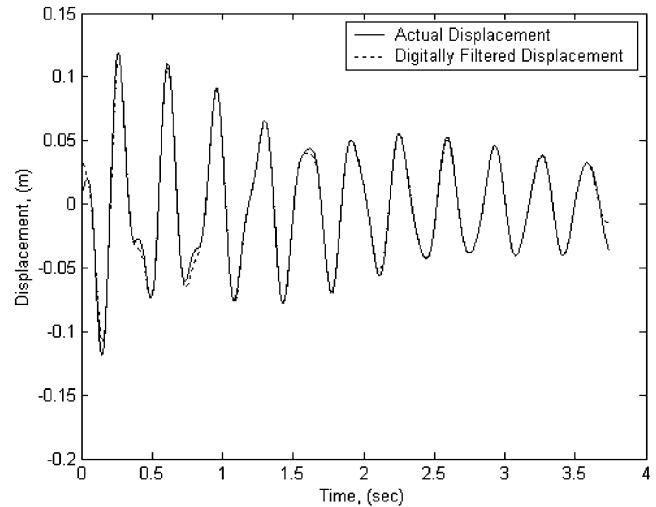

Fig. 3.   Digitally filtered displacement time-history.

cutoff frequency for the filter can be estimated from the knowledge of approximate zero-wind speed frequencies of the dynamic system. The actual (noise free) displacement and the filtered displacement are plotted in Fig. 3. The filtered displacement data were used to generate velocity and acceleration time-histories by finite difference formulation, as shown in Figs. 4 and 5, respectively.

It can be seen from Figs. 3–5 that the digitally *filtered displacement* and the numerically obtained *velocity* and *acceleration* time-histories deviate from the actual time-histories at the two extreme ends of the total time range. This is an inherent error for zero-phase digital filtering using MATLAB function. To circumvent the misfit at the two ends, a 'windowing' method was applied which used only the middle portion of each of the three time-histories for system identification. A 'window', which discards the first and last quarter of each time-history, was found to be suitable for obtaining parameters through system identification. Thus, only the middle half

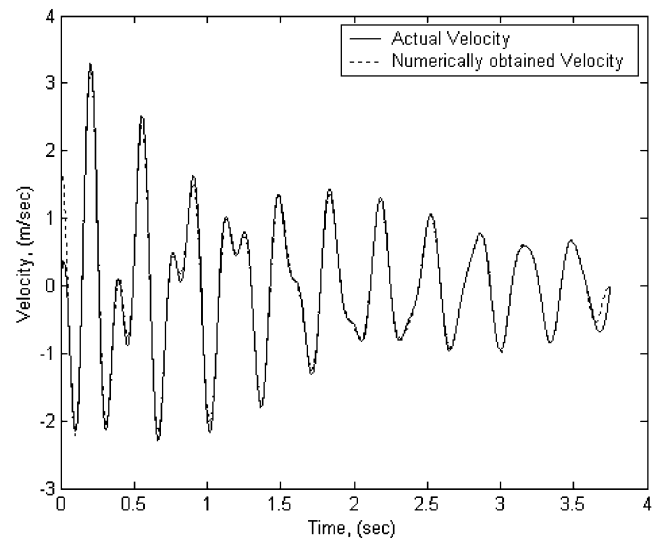Fig. 2.   Noisy displacement time-history.

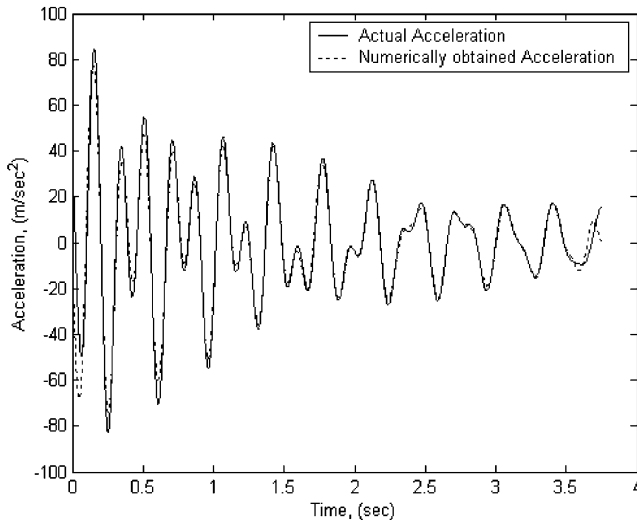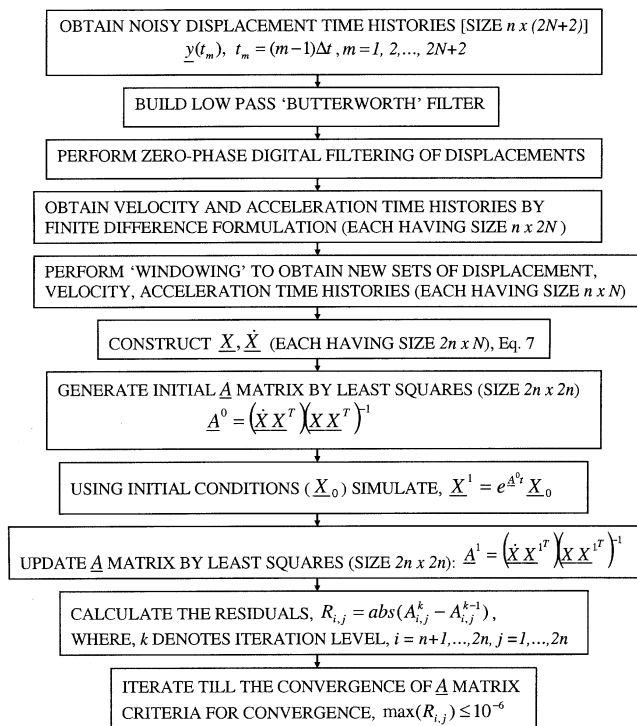Fig. 4.   Numerically obtained velocity time-history.

Fig. 5. Numerically obtained acceleration time-history.

of each time-history is considered for extracting elements of the *A* matrix by the ILS approach. The *A* matrix obtained for zero wind case, will give the C^{mech} and K^{mech} matrices. The *A* matrix obtained for non-zero wind speeds, will give the C^{eff} and K^{eff} matrices. After estimating the elements of these matrices, the frequency-dependent flutter derivatives can be calculated from Eqs. (4)–(6).

2.4. Algorithm for the iterative least squares (ILS) approach

Based on the ILS approach, a computer code has been developed to identify the elements of *A* matrix from noisy displacement time-histories. The ILS approach is effectively described by the following algorithm

OBTAIN NOISY DISPLACEMENT TIME HISTORIES [SIZE *n x (2N+2)*]
$\underline{y}(t_m)$, $t_m = (m-1)\Delta t$, $m = 1, 2, ..., 2N+2$

↓

BUILD LOW PASS 'BUTTERWORTH' FILTER

↓

PERFORM ZERO-PHASE DIGITAL FILTERING OF DISPLACEMENTS

↓

OBTAIN VELOCITY AND ACCELERATION TIME HISTORIES BY FINITE DIFFERENCE FORMULATION (EACH HAVING SIZE *n x 2N*)

↓

PERFORM 'WINDOWING' TO OBTAIN NEW SETS OF DISPLACEMENT, VELOCITY, ACCELERATION TIME HISTORIES (EACH HAVING SIZE *n x N*)

↓

CONSTRUCT $\underline{X}, \underline{\dot{X}}$ (EACH HAVING SIZE *2n x N*), Eq. 7

↓

GENERATE INITIAL $\underline{A}$ MATRIX BY LEAST SQUARES (SIZE *2n x 2n*)
$$\underline{A}^0 = \left(\underline{\dot{X}}\,\underline{X}^T\right)\left(\underline{X}\,\underline{X}^T\right)^{-1}$$

↓

USING INITIAL CONDITIONS ($\underline{X}_0$) SIMULATE, $\underline{X}^1 = e^{\underline{A}^0 t}\underline{X}_0$

↓

UPDATE $\underline{A}$ MATRIX BY LEAST SQUARES (SIZE *2n x 2n*): $\underline{A}^1 = \left(\underline{\dot{X}}\,\underline{X}^{1T}\right)\left(\underline{X}\,\underline{X}^{1T}\right)^{-1}$

↓

CALCULATE THE RESIDUALS, $R_{i,j} = abs(A_{i,j}^k - A_{i,j}^{k-1})$, WHERE, *k* DENOTES ITERATION LEVEL, $i = n+1, ..., 2n$, $j = 1, ..., 2n$

↓

ITERATE TILL THE CONVERGENCE OF $\underline{A}$ MATRIX CRITERIA FOR CONVERGENCE, $\max(R_{i,j}) \leq 10^{-6}$

3. Experimental set-up

A three-DOF elastic suspension system (Fig. 6) has been developed and built for testing at the Wind Simulation and Testing (WiST) Laboratory, Department of Aerospace Engineering, Iowa State University. The schematic diagram of the system is shown in Fig. 7, which illustrates different views of the system and their corresponding dimensions. This system enables simultaneous vertical, horizontal, and torsional motion of the suspended model and captures the effect of coupling between different degree of freedom of a flexible structure immersed in a dynamic flow field. The system utilizes pneumatic bushings that glide along polished steel shafts in the vertical and horizontal directions of motion. Two torsional assemblies on each side are used to generate torsional motion of the model. Each assembly can be housed in a built-up aluminum box having dimension, $300 \times 150 \times 64$ mm (shown in Fig. 7) to give it a compact finish. Vibration frequencies of the system are tuned with combination of springs. System damping is low due to the low-friction pneumatic bushings, restriction of coil spring wire to small diameters, and highly polished stainless steel guide shafts. Relatively large displacements can be generated by the suspension system.

Force measurements were accomplished with strain gage force transducers applied to four of the spring attachment points, two vertical and two horizontal. The force transducers that were used are miniature load cells with 11.34 kg (25 lb) capacity. These load cells were chosen based on their light-weight and compact size. The torque-sensor, which has a capacity of 1.152 kg-m (100 lb-in), was fixed to the back wall of one of the two torsional assemblies. The front end of the torque sensor was connected to the rigid bottom bar, and thus could measure the torque produced by the pair of springs. The torsional assemblies allowed the model to undergo rotational motion under wind loading and the torque-sensor measured the aerodynamic moment caused by the motion. LabView (National Instruments) was used for data acquisition from wind tunnel experiments.

For wind tunnel testing, a section model of NACA 0020 airfoil was mounted on the three-DOF elastic suspension system. The airfoil was symmetric about its chord and had a thickness-to-chord ratio of 20%. The Styrofoam airfoil model had a chord length of 314 mm. The airfoil model was 550 mm long, with two elliptical Plexiglas end plates to reduce aerodynamic end effects. The model was built with foam and wrapped around with fiberglass to simulate the smooth airfoil skin. A hollow aluminum shaft ran through the model. It was supported on high precision ball bearings at two ends. The shaft was connected to the torsional assembly at both ends to facilitate the rotational DOF. The center-of-gravity of the model coincided with the elastic axis to avoid static imbalance.
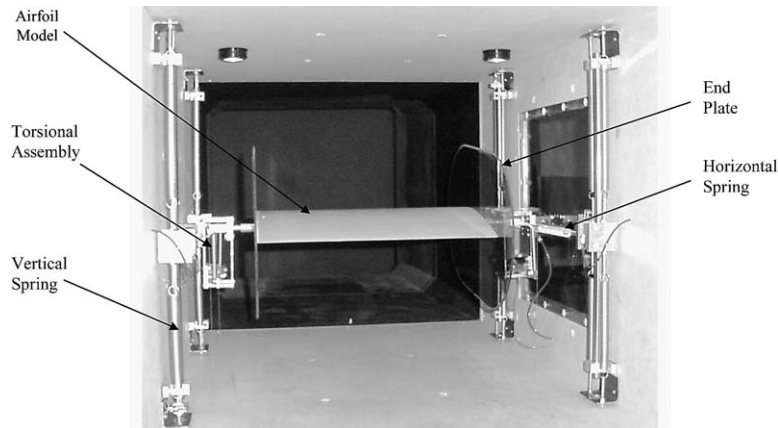
Fig. 6. Three-DOF elastic suspension system inside Bill James wind tunnel test section, WiST Laboratory.

Isometric View   Top View
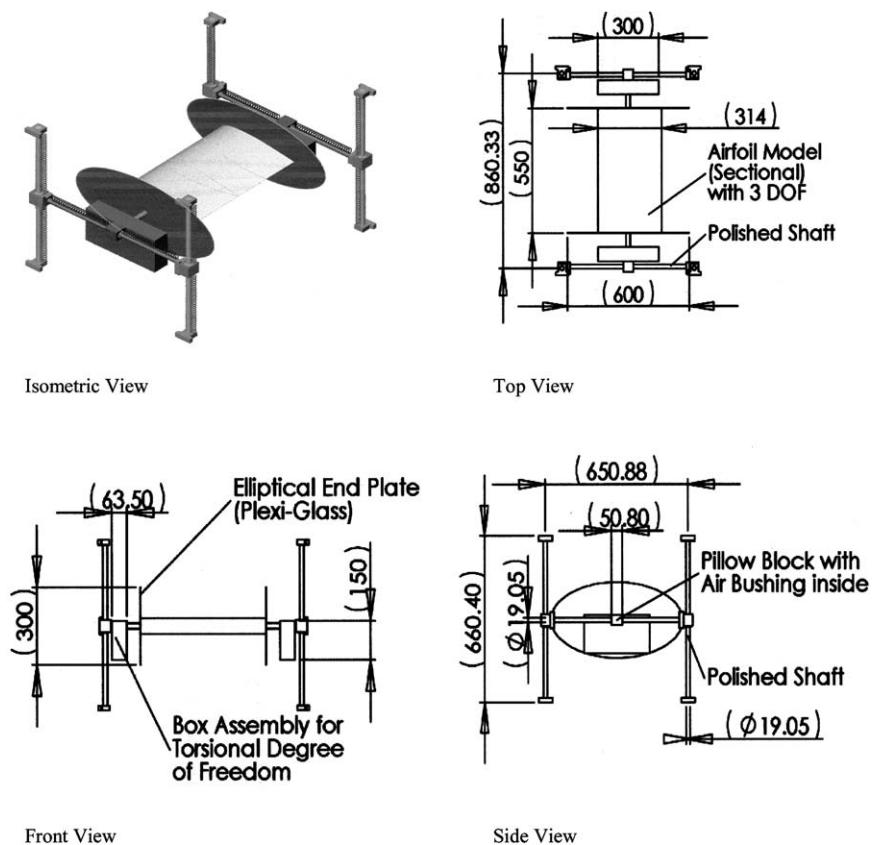
Front View   Side View

Fig. 7. Schematic diagram of three-DOF elastic suspension system (all dimensions are in mm).

While designing the elastic suspension system and the airfoil model, the mechanical frequencies for the vertical, lateral, and torsional motions were carefully chosen. The desired frequencies were then obtained by a suitable combination of springs. The mechanical frequencies of the dynamic system were designed close to 1.8, 2.5, and 3.5 Hz for the lateral, vertical, and torsional-DOF, respectively. These frequencies were selected such that they were distinct from each other and provide the maximum reduced velocity desired in the experiment corresponding to a pre-selected wind speed below the estimated flutter speed of the model. The frequency along the vertical DOF was used for the calculation of the reduced velocities.

4. Results and discussion

4.1. Numerical simulations

ILS method was programmed and tested for typical one, two, and three-DOF dynamic systems whose mass,

stiffness, and damping matrices were assumed. The purpose of the numerical simulation was to determine the percentage of error for the elements of the damping and stiffness matrices, which were extracted from noisy displacement time-histories. Cases with different noise-to-signal ratios were considered during numerical simulation. The average errors for the stiffness and damping terms are given in Table 1, where errors in parameter estimation for a two-DOF system were compared with the MITD [3] method, because its algorithm was readily available. The average percentage errors for two-DOF parameters extracted using the ILS method for 10% noise are significantly less than those using the MITD method for 5% noise. As expected for the numerical simulations, the errors in diagonal terms are less compared to the errors in non-diagonal terms for the stiffness and damping matrices. The parameter errors increase with increasing number of degree of freedom. It is evident from Table 1 that the errors for three-DOF parameters for the 5% noise case are more than the errors for two-DOF parameters for the 20% noise case. Thus, parameters extracted for a two-DOF model in a turbulent flow is more accurate than parameters extracted for a three-DOF model in comparatively less turbulent flow. This particular phenomenon bolsters the concept of generating all 18 flutter derivatives from different two-DOF combinations instead of performing a single three-DOF testing. The current method is capable of generating good estimates of parameters even for high noise-to-signal ratio for one and two-DOF systems (e.g. error in extracted parameters is much less than 10% for 20% noise). For three DOF system, the method works satisfactorily for moderate noise level (e.g. error in extracted parameters is less than 10% for 10% noise).

From the numerical simulations, it is evident that the ILS method estimates the parameters more accurately than the MITD method for a given noise level. Thus, the ILS method can extract parameters even at relatively high noise level, which can occur for turbulent flows or inadequate resolution of transducers. Moreover for MITD method, the time shifts N1 and N2 [5] cannot be arbitrarily chosen because they affect the accuracy of parameter extraction. Since the ILS method does not involve N1 and N2, the accuracy of the estimated parameters are independent of the estimated values of N1 and N2. Also the ILS method estimates the elements of C^{eff} and K^{eff} matrices directly instead of obtaining them from complex eigenvalues and eigenvectors, thereby reducing mathematical complexity.

4.2. Experimental results

All 18 flutter derivatives were obtained for the NACA 0020 airfoil model by using the ILS approach. For comparison, all the possible DOF combinations were tested in the wind tunnel. Thus, the estimates of flutter derivatives obtained from different combinations of DOF could be compared. The versatility of the three-DOF elastic suspension system remains in the fact that all possible combinations (e.g. 1-DOF, 2-DOF, and 3-DOF) could be tested by restraining one or more DOF as required for a particular experimental set-up. Thus, the accuracy of a particular flutter derivative could be determined by matching the results from more than one set of DOF combinations. Table 2 shows all possible DOF combinations and the flutter derivatives that were obtained from each combination.

For wind tunnel experiments, a sampling rate of 800 Hz was used for obtaining the vertical, lateral, and torsional time-histories at zero and different non-zero wind velocities. Number of sample points, $2N + 2$ was taken as 3002 for each displacement time-history. This number was considered to keep the amplitude levels of decaying sinusoidal motions above a certain fixed level to avoid high background noise ratio. An ensemble of 10 time-histories was taken for each wind speed. The ILS program was used for processing the data. The cut-off frequency for the Butterworth filter was chosen to be slightly higher than the maximum zero-wind speed natural frequency of the dynamic system (i.e. 3.5 Hz for the three-DOF case). A cut-off frequency chosen between 5 and 6 Hz was found to work effectively for filtering purposes of the three-DOF noisy displacement time-histories. Finite difference formulation (central-difference with truncation error TE = $O[(\Delta t)^2]$) was used to obtain the velocity and acceleration time-histories from the

Table 1
Average percentage errors for numerical simulations

Case	Noise-to-signal ratio	Diagonal stiffness terms	Non-diagonal stiffness terms	Diagonal damping terms	Non-diagonal damping terms
1-DOF (ILS)	20%	0.02	–	1.67	–
2-DOF (MITD)	5%	0.19	2.22	0.81	2.02
2-DOF (MITD)	10%	0.37	4.47	1.60	2.92
2-DOF (ILS)	10%	0.06	0.82	0.56	1.41
2-DOF (ILS)	20%	0.13	0.96	2.01	5.04
3-DOF (ILS)	5%	0.44	1.51	2.55	5.99
3-DOF (ILS)	10%	0.89	2.34	4.83	8.43

Table 2
DOF combinations and corresponding flutter derivatives obtained

Case	DOF combination	Flutter-derivatives extracted
1	1-DOF vertical (V)	H1∗, H4∗
2	1-DOF torsional (T)	A2∗, A3∗
3	1-DOF lateral (L)	P1∗, P4∗
4	2-DOF vertical and torsional (V&T)	H1∗, H2∗, H3∗, H4∗, A1∗, A2∗, A3∗, A4∗
5	2-DOF vertical and lateral (V&L)	H1∗, H4∗, H5∗, H6∗, P1∗, P4∗, P5∗, P6∗
6	2-DOF lateral and torsional (L&T)	P1∗, P4∗, P2∗, P3∗, A2∗, A3∗, A5∗, A6∗
7	3-DOF	All 18 flutter derivatives

digitally filtered displacement data. 'Windowing' operation was performed and middle half of each time-history was considered for extracting elements of the A matrix by the ILS approach.

The convergence of A matrix was obtained based on the residuals $R_{i,j}$ which were taken as absolute values of differences between elements of A matrices obtained from two consecutive iteration levels as shown in the algorithm. Criteria for convergence was to have the maximum residual $\max(R_{i,j})$ less than or equal to 10^{-6}. While extracting elements of the state matrix from the experimental data, it took ILS method five to seven iterations to converge based on the above criteria. After estimating the elements of A matrix at zero wind speed and several non-zero wind speeds, the frequency-dependent flutter derivatives were calculated using Eqs. (4)–(6).

The flutter derivatives thus obtained from different DOF combinations are plotted in Figs. 8–10. All the
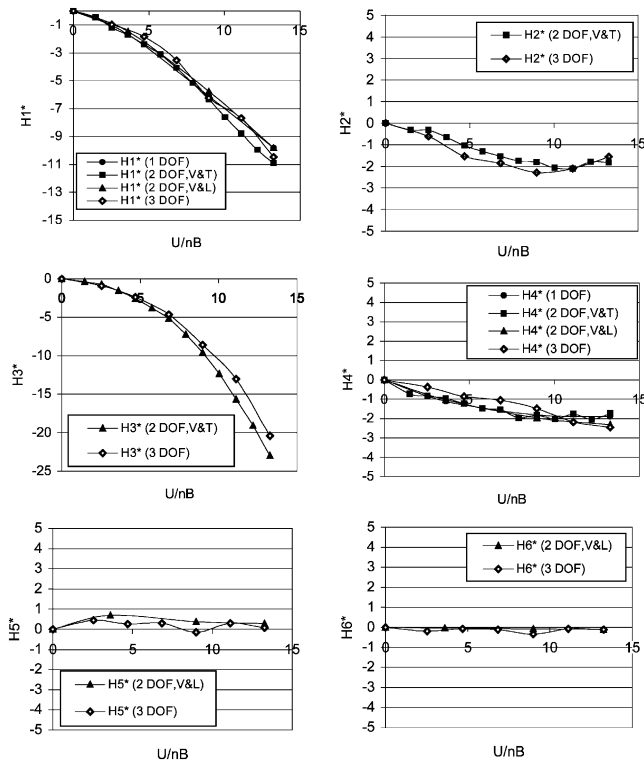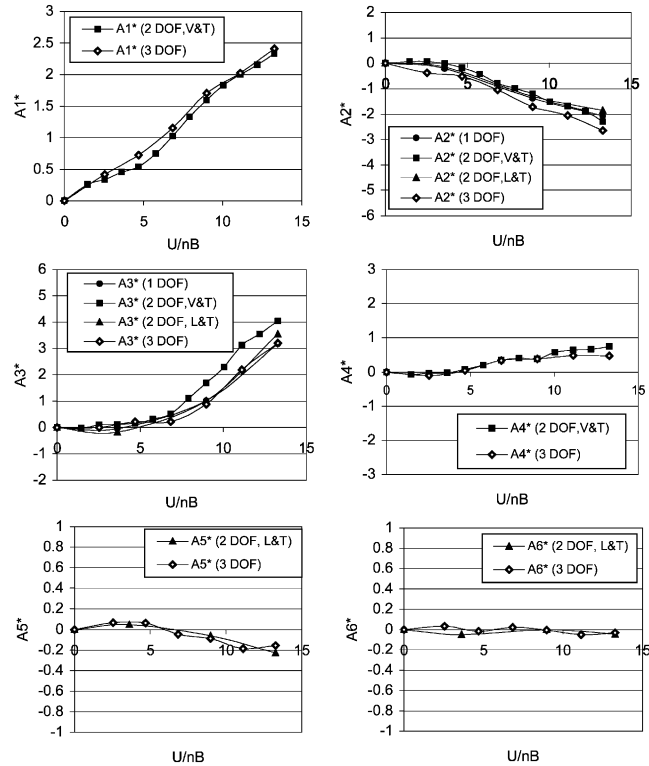

Fig. 9.   Torsional flutter derivatives (A_i^*, i = 1,2, ..., 6).

flutter derivatives were calculated for a range of reduced velocities. The vertical frequency of the dynamic system was used to obtain the non-dimensional reduced velocity for all cases. Good agreement is seen between vertical and torsional flutter derivatives H1∗, H2∗, H3∗, H4∗, A1∗, A2∗, A3∗, A4∗ obtained from 1-DOF, 2-DOF and 3-DOF testing. The lateral derivative P1∗, which represents the damping of lateral displacement, shows very good agreement when obtained from different DOF combinations. Though there are some deviations at isolated points, the trends for the other derivatives, obtained from various DOF combinations, namely, H5∗, H6∗, A5∗, A6∗, P2∗, P3∗, P4∗, P5∗, P6∗ are consistent. These isolated variations, especially for some of the lateral derivatives, need further investigation. Flutter derivatives extraction from three-DOF testing is comparatively more difficult than obtaining them from one-
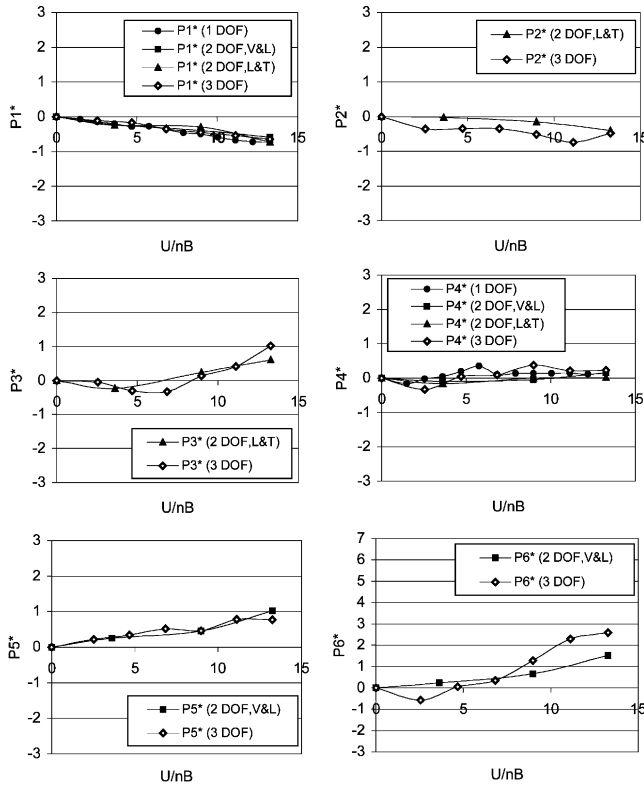

Fig. 8.   Vertical flutter derivatives (H_i^*, i = 1, 2, ..., 6).

Fig. 10. Lateral flutter derivatives (P_i^*, $i = 1, 2, ..., 6$).

DOF and two-DOF tests. Thus, it is recommended to extract all 18 derivatives for a section model by performing three different sets of two-DOF testing namely, vertical-torsional, vertical-lateral, and lateral-torsional.

5. Conclusions

Work in the field of identifying all 18 flutter derivatives for a section model has been limited. This motivated the development of a new system identification method (iterative least squares method or ILS method) to efficiently extract all 18 flutter derivatives. The identification technique used experimentally obtained free-vibration displacement time-histories generated by a section model supported by a three-DOF elastic suspension system in the wind tunnel test section. Numerical simulations demonstrated the efficiency of the ILS method. It was evident that the errors in parameter extraction increased when number of DOF increased from two to three. The numerical simulations showed that the ILS method was capable of generating good parameter estimates for one- and two-DOF testing with high noise-to-signal ratio and for three-DOF testing with moderate noise-to-signal ratio. All 18 flutter derivatives for an airfoil section model were extracted using the ILS method to demonstrate the extraction technique. The accuracy of a particular flutter derivative was determined by matching the results obtained from all possible DOF combi-

nations. Trends of the flutter derivatives coincided when obtained from more than one set of DOF combination. Flutter derivatives extraction from three-DOF testing was comparatively more difficult than obtaining them from one-DOF and two-DOF tests. Performing three different sets of two-DOF testing namely, vertical-torsional, vertical-lateral, and lateral-torsional, instead of three-DOF testing, would be an efficient technique for accurate extraction of all 18 derivatives for a section model.

6. Dedication

This paper is dedicated to the late Professor Robert H. Scanlan, The Johns Hopkins University, Baltimore, MD, USA, who had been a mentor and Ph.D. dissertation advisor of co-author, Partha P. Sarkar. Professor Scanlan had provided the initial inspiration and motivation for the work that is presented here.

References

[1] Scanlan RH, Tomko JJ. Airfoil and bridge deck flutter derivatives. J Eng Mech Div, ASCE 1971;97(6):1717–33.
[2] Scanlan RH. The action of flexible bridges under wind. I: Flutter theory. J Sound Vibr 1978;60(2):187–99.
[3] Sarkar PP. New-identification methods applied to the response of flexible bridges to wind. PhD thesis. Baltimore, MD: The Johns Hopkins University, 1992.
[4] Sarkar PP, Jones NP, Scanlan RH. System identification for estimation of flutter derivatives. J Wind Eng Ind Aerodyn 1992;41-44:1243–54.
[5] Sarkar PP, Jones NP, Scanlan RH. Identification of aeroelastic parameters of flexible bridges. J Eng Mech ASCE 1994;120(8):1718–42.
[6] Imai H, Yun CB, Maruyama O, Shinozuka M. Fundamentals of system identification in structural dynamics. Prob Eng Mech 1989;4:162–73.
[7] Hsia TC. On least squares algorithms for system parameter identification. IEEE Trans Autom Contr 1976;21(1):104–8.
[8] Yamada H, Ichikawa H. Measurement of aerodynamic parameters by extended Kalman filter algorithm. J Wind Eng Ind Aerodyn 1992;42:1255–63.
[9] Diana G, Cheli F, Resta F. Time domain aeroelastic force identification on bridge decks. In: Proce 9th Int Conf Wind Eng, New Delhi, India. Wiley Eastern Ltd; 1995. p. 938–49.
[10] Iwamoto M, Fujino Y. Identification of flutter derivatives of bridge deck from free vibration data. J Wind Eng Ind Aerodyn 1995;54/55:55–63.
[11] Jones NP, Shi T, Ellis JH, Scanlan RH. System-identification procedure for system and input parameters in ambient vibration surveys. J Wind Eng Ind Aerodyn 1995;54/55:91–9.
[12] Jakobsen JB, Hjorth-Hansen E. Determination of the aerodynamic derivatives by a system identification method. J Wind Eng Ind Aerodyn 1995;57:295–305.
[13] Brownjohn JMW, Jakobsen JB. Strategies for aeroelastic parameter identification from bridge deck free vibration data. J Wind Eng Ind Aerodyn 2001;89:1113–36.
[14] Gu M, Zhang R, Xiang H. Identification of flutter derivatives of bridge decks. J Wind Eng Ind Aerodyn 2000;84:151–62.
[15] Zhu LD, Xu YL, Zhang F, Xiang HF. Tsing Ma bridge deck

under skew winds. Part II: Flutter derivatives. J Wind Eng Ind Aerodyn 2002;90:807–37.

[16] Singh L, Jones NP, Scanlan RH, Lorendeaux O. Simultaneous identification of 3-dof aeroelastic parameters. In: Proc 9th Int Conf Wind Eng, New Delhi, India. Wiley Eastern Ltd; 1995. p. 972–81.

[17] Chen A, He X, Xiang H. Identification of 18 flutter derivatives of bridge decks. J Wind Eng Ind Aerodyn 2002;90:2007–22.

[18] Ibrahim SR, Mikulcik EC. The experimental determination of vibration parameters from time responses. The Shock and Vibration Bulletin 1976;Bulletin 46:187–96.